博 士 論 文

Antibacterial potential of colloidal platinum nanoparticles against *Streptococcus mutans*
(ストレプトコッカスミュータンスに対する白金ナノコロイドの抗菌性)

令和０４年０３月申請

北海道大学
大学院歯学院口腔医学専攻

張洪波
Zhang Hongbo

INTRODUCTION

Dental caries is a disease of the teeth's hard tissue demineralization, caused by constant exposure of free sugar to the dental biofilm that alters the ecological balance towards caries ecological disorders[1-3]. Carious lesions in adults mainly occur on proximal surfaces or are related to existing restorations (secondary caries) in permanent teeth[4]. In clinical situations, remaining bacteria in the cavity pose potential risks of secondary carious lesions[5]. Caries around restorations is usually caused by the accumulation of biofilm (dental plaque) above and at the restoration edge and the release of acids and enzymes produced by the cariogenic bacteria during fermentation[6,7]. New generations of restorative materials with antibacterial are being developed to prevent the development of secondary caries. For instance, in the last decades, there has been an increased interest in employing metallic nanoparticles as an antibacterial agent in restorative materials[8-10].

Several metallic compounds have been used for centuries as antibacterial agents[11]. These metallic agents demonstrate efficacies by damaging bacterial cell walls, producing reactive oxygen species, or inactivating intracellular proteins[12]. The potential of such inorganic compounds depends on the extent of their contact surfaces, and therefore, a compound with a larger surface area exhibits superior performance[13]. Metallic nanoparticles have demonstrated substantial antimicrobial sensitivity because these nanoparticles inherently have larger surface areas, allowing a broader gamut of interactions with other organic and inorganic molecules[11]. Chwalibog *et al.* reported that 50 ppm hydrocolloid of platinum nanoparticles (PtNPs), produced from high purity

platinum, manifested excellent antibacterial activity by successfully disintegrating the cell walls of *Staphylococcus aureus* and *Candida albicans*[14]. Tahir *et al.* showed that PtNPs exhibit potent antibacterial activity against antibiotic-resistant *Pseudomonas aeruginosa* and *Bacillus subtilis*[15]. Hashimoto *et al.* found that PtNPs adhere to the surfaces of *Streptococcus mutans* (*S. mutans*) and inhibit biofilm formation[16]. Platinum has been certified safe as a food additive, and several commercial products supplemented with platinum nanoparticles as antioxidants, including mineral water, yogurt, gum, candies, mouthwash, and skin lotion, are marketed in developed countries[17].

Colloidal platinum nanoparticles (CPNs), which consist of metallic nanomaterials synthesized from the colloidal suspension of platinum particles, are effective in reducing inflammation[17,18] and preventing apoptosis[19]. CPNs have also been found to delay the aging process because CPNs can act as antioxidants by scavenging reactive oxygen species[20]. The successful outcome of CPNs in potentially treating diseases related to oxidative stress and aging has been studied[20,21]. In the field of dental biomaterials, CPNs were found to enhance the bonding performance of 4-META/MMA-TBB-based resin cement to sound dentin[22-24]. However, caries-affected dentin particularly proved to be a challenge to the bonding outcome of a restorative material as the complete removal of cariogenic bacteria can hardly be confirmed by a clinician[25].

Surprisingly, no literature has tested the efficacy of CPNs against one of the causative cariogenic microorganisms, *S. mutans*. Therefore, the objective of this study is to assess the antibacterial effect of three types of CPNs on *S. mutans*. The null hypothesis was that the three types of CPNs would not affect the growth and biofilm formation of *S.*

mutans.

MATERIALS AND METHODS

Bacterial strain and culture conditions

Streptococcus mutans 109c (*S. mutans* 109c, wildtype, serotype c)[26] was cultured overnight at 37°C in brain heart infusion (BHI) broth (Becton, Dickinson and Company, Sparks, MD, USA) under anaerobic conditions (80% N_2, 10% H_2, 10% CO_2). The resulting bacterial suspension was adjusted to an optical density at 600 nm (OD_{600}) of 1.0 using a spectrophotometer (Bio-Rad Smartspec™ plus, Hercules, CA, USA) for further use.

Determination of antibacterial activity

Three different formulations of the CPNs (APt company, Tokyo, Japan) were used in this study (Table 1). The pH values of these three CPNs were measured by pH meter (392R, AS ONE Corporation, Osaka, Japan). The CPNs were diluted with BHI broth to various concentrations (0.4–0.9 mM). The concentration of platinum in the solution ranged from 80 to 180 ppm (manufacturer's information). Sterile water and suspended bacteria were used as the control group.

The antibacterial activity of six different concentrations (0.4, 0.5, 0.6, 0.7, 0.8, and 0.9 mM) of each of the CPNs on *S. mutans* was initially tested. For the assessment, 20 µL *S. mutans* suspension was mixed with various concentrations of innovative solutions (980 µL) and incubated at 37°C for 24 h. Following CPNs treatment of each group, dilution series (10^{-1}–10^{-5}) were prepared using a sterilized saline solution, and 100 µL of

each dilution was spread onto BHI agar plates and the plates incubated at 37°C for 48 h. The number of bacterial colonies on each BHI agar plate was obtained using a bacterial colony counter (Count™, Heathrow Scientific, Vernon Hills, IL, USA). The bacterial concentration in samples after co-culturing (*N*, CFU/mL) was calculated by using Eq. (1), whereas the antibacterial rate was determined by using Eq. (2):

$$N=(C\times d\times 1000)/l \quad (1)$$

$$Antibacterial\ rate=\left(N_{\text{control}}-N_{\text{material}}\right)/N_{\text{control}}\times 100\% \quad (2).$$

In Eq. (1), *C* represents the average colony count on the plates, *d* is the dilution factor with *d*=50 in this study, and *l* is the volume of the bacterial suspension used in the samples with a value of *l*=100 in this study. In Eq. (2), N_{control} and N_{material} are the average colony counts for the control (water) and CPNs groups, respectively[27]. According to the National Standard of China (GB/T 4789.2-2010), an antibacterial rate≥99% means that the sample has substantial antibacterial activity, and an antibacterial rate≥90% indicates that the sample has antibacterial activity[28]. Experiments were performed in triplicate.

Growth inhibition study

Growth inhibition analysis was performed to determine the inhibition kinetics of CPNs against *S. mutans*. The three CPNs were added to bacterial suspensions to a final concentration of 0.7 mM (the value was determined previously, as described before). The suspensions were incubated at 37°C under anaerobic conditions. After 1, 2, 3, 4, 5, and 6 h incubation, 100 µL of each suspension was serially ten-fold diluted and spread onto BHI agar plates. The number of viable bacterial colonies was counted after 48 h. The experiment was performed in triplicate.

Live/dead staining for visualization of S. mutans *viability*

S. mutans was incubated at 37°C for 24 h. Bacteria in the logarithmic growth phase (concentration OD_{600}=1.0) were treated with 0.7 mM CPNs for 24 h. Sterile water was used as the control group. Bacterial suspensions were stained using the Live/Dead BacLight Bacterial Viability kit L7012 (Molecular Probes, Eugene, OR, USA) for 15 min in the dark at room temperature. The kit consists of Syto 9, which stains all cells green, and propidium iodide, which stains dead cells red because these cells have a damaged cell membrane. Samples were observed using a fluorescence microscope (BZ-X800, Keyence, Osaka, Japan). The experiment was performed in triplicate. Images were analyzed using Image-Pro Plus 5.0.

Effects of CPNs on S. mutans *morphology*

S. mutans were incubated in the presence of 0.7 mM CPNs for 24 h. The samples were harvested by centrifugation, washed twice with sterilized phosphate-buffered saline (PBS), and fixed in 2.5% glutaraldehyde overnight. The attached bacteria were adhered to glass coverslips, dehydrated serially in ethanol (50% for 10 min, 80% for 10 min, and 100% for 20 min), and air-dried overnight. Samples were then sputter-coated with gold-palladium and examined with a scanning electron microscope (SEM, S-4800, Hitachi, Tokyo, Japan).

Biofilm analysis

CPNs were diluted with BHI broth containing 1% sucrose to various concentrations (0–0.9 mM). *S. mutans* strains (OD_{600}=1.0) were then cultured in sterile 96-well microtiter

plates in BHI broth (containing CPNs and 1% sucrose) at 37°C for 24 h. Sterile water was used as the control group. After incubation, the planktonic bacteria were removed, and the wells were washed three times with PBS. The biofilm was fixed with 100 µL 99.99% methanol per well, and after 15 min, microplates were aspirated and air-dried. Crystal violet (CV) staining was used to measure bacterial biofilm formation[29]. One hundred microliters CV was added to stain the biofilm and incubated at 37°C for 5 min. The excess stain was removed by placing the microplate under running tap water. After air-drying the microplates, dye bound to the adherent cells was resolubilized with 100 µL 33% (v/v) glacial acetic acid per well. The optical density of each well was measured at 570 nm using a microplate reader (Model 3550, Bio-Rad). Biofilm formation by bacteria after co-culturing with CPNs was calculated by Eq. (3):

$$P = {O_{\text{material}}}/{O_{\text{control}}} \times 100\% \quad (3).$$

In Eq. (3), O_{control} and O_{material} are the optical densities for the control (water) and CPNs groups, respectively.

*Live and dead staining (*S. mutans *biofilm viability test)*

For the biofilm viability test, *S. mutans* were grown in sterile 24-well microtiter plates with glass cover slides (Matsunami, Chiba, Japan) for 24 h with BHI broth containing 1% sucrose. Sterile water was used as the control group. After exposure to 0.5 mM CPNs for 24 h, biofilms were stained with Live/Dead BacLight Bacterial Viability kit L7012 (Molecular Probes). Sample fluorescence was observed using the fluorescence microscope (BZ-X800, Keyence) at 488 and 543 nm excitation wavelengths. The experiment was performed in triplicate.

Effect of CPNs on S. mutans *biofilm morphology*

SEM was used to observe biofilms formed overnight in 24-well plates with glass cover slides at the bottom of each well. Before SEM imaging, the biofilm was treated with 0.5 mM CPNs for 24 h at 37°C. The CPNs-containing medium was removed, and the wells were gently washed twice with sterilized distilled water and fixed in 2.5% glutaraldehyde overnight. The fixed samples adhered to glass coverslips were dehydrated serially in ethanol (50% for 10 min, 80% for 10 min, and 100% for 20 min) and finally air-dried in a desiccator overnight. The samples were sputter-coated with gold-palladium and examined by SEM (S-4800, Hitachi).

Statistical analysis

Statistical analyses were carried out with SPSS 19.0 (SPSS, Inc.). The normality of the data was checked with the Shapiro-Wilk test and the homogeneity with Levene's test. Since the data were normal and homogeneous, the one-way ANOVA with Dunnett's multiple comparison test was used to determine the statistical significance ($p<0.05$) between different groups.

RESULTS

Determination of antibacterial activity

Fig. 1 shows the changes in the antibacterial rate of CPNs on *S. mutans*. The antibacterial rate of 0.7 mM PAA-Pt was about 91.5% (>90%) while the antibacterial rate of 0.7 mM C-Pt and 0.7 mM C-CyD-Pt were only about 69.0% (<90%). This result suggests that 0.7 mM PAA-Pt is antibacterial material, whereas 0.7 mM C-Pt and 0.7 mM C-CyD-Pt are

not according to the National Standard of China GB4789.2.

Growth inhibition study

Fig. 2 shows the growth-inhibitory curves of the three types of CPNs at 0.7 mM against *S. mutans*. The three types of CPNs showed potent antibacterial activity up to 6 h. The PAA-Pt group demonstrated the most potent antibacterial activity with no significant increase in the number of bacteria observed up to 6 h.

Live/dead staining for visualization of S. mutans *viability*

Typical live/dead images of *S. mutans* exposed to the three CPNs at 0.7 mM for 24 h are shown in Fig. 3. The number of bacteria detected in the control group (i.e., water-only sample) was the largest. In contrast, the groups containing CPNs showed fewer live bacteria than the control group. In particular, the PAA-Pt group showed the lowest number of live bacteria among these groups.

Morphology changes to S. mutans

As shown in Fig. 4, *S. mutans* cells in the control group exhibited smooth surfaces, whereas cells exposed to 0.7 mM CPNs for 24 h had a rough appearance. Additionally, CPNs-exposed *S. mutans* displayed an elongated morphology when compared with bacteria from the control group. Moreover, SEM images of *S. mutans* exposed to the three types of CPNs showed two or more ring-like structures along their circumferences[30].

Concentration-dependent inhibition of S. mutans *biofilm formation by CPNs*

Formation of *S. mutans* biofilm was reduced by PAA-Pt group at concentrations >0.5 mM, whereas C-Pt and C-CyD-Pt groups showed a biofilm inhibitory effect at

concentrations higher than 0.8 mM (Fig. 5).

Live/dead staining for visualization of S. mutans *biofilm formation*

Fig. 6 shows the live/dead staining results at 0.5 mM CPNs on *S. mutans* biofilm formation. PAA-Pt group showed the most substantial inhibitory effect on biofilm formation, whereas C-Pt and C-CyD-Pt groups generated a weaker inhibitory effect. Exposure of *S. mutans* biofilms to PAA-Pt, C-Pt, and C-CyD-Pt groups resulted in more dead bacteria when compared with that of the water (control) sample.

Morphology changes to S. mutans *biofilm*

As shown in Fig. 7A–D, reduction in biofilm formation by *S. mutans* mainly occurred when exposed to 0.5 mM PAA-Pt group. The anti-biofilm activity of C-Pt and C-CyD-Pt groups was weaker than that of the PAA-Pt group but more robust than the water sample (control). As shown in Fig. 7F–H, bacteria treated with PAA-Pt, C-Pt and C-CyD-Pt demonstrated granular features on their surfaces. *S. mutans* exposed to CPNs also showed an elongated morphology compared with bacteria from the control sample (Fig. 7). These observations corroborate the observed morphological changes to *S. mutans* observed in Fig. 4.

DISCUSSION

This study showed that three different CPNs inhibited the growth of *S. mutans*. Therefore, the tested null hypothesis had to be rejected. According to our knowledge, the findings of this study are the first to demonstrate the inhibitory effect of CPNs on *S. mutans* biofilm formation. PAA-Pt exhibited the most significant inhibitory effect ($p<0.05$) on the biofilm

formation of *S. mutans* among the tested groups. In the present study, 0.7 mM PAA-Pt showed the highest antibacterial activity among these three 0.7 mM CPNs, with an antibacterial rate of 91.5% (Fig. 1). This result was supported by the live/dead cell staining images presented in Fig. 3, where the PAA-Pt concentration of 0.7 mM showed the lowest fluorescence of live and dead cells.

The three types of CPNs have the same concentration of platinum (1 mM); however, the other components present in the nanoparticles differed: PAA-Pt contains 1.16% polyacrylic acid, C-Pt contains 0.29% sodium citric acid, and C-CyD-Pt contains 0.29% sodium citric acid and 0.3% cyclodextrin. Studies have shown that sodium citric acid is an antibacterial agent[31,32]. Yamaguchi *et al.* report that a citric acid solution showed antibacterial activity toward all bacteria tested[32]. There are no reports on the antibacterial activities of cyclodextrin and polyacrylic acid. Nonetheless, the PAA-Pt group showed the highest antibacterial activity. We speculated that the observed different antibacterial activities of the three CPNs might be attributed to their different compositions and combinations of chemicals. We speculate that polyacrylic acid is a mucoadhesive, and it may be helped the platinum to bind to the bacterial cells so that PAA-Pt showed the highest antibacterial activity. In the current study, only CPNs formulations were used, and the individual ingredients were not tested, and hence, further research is necessary to evaluate the role of each component in inhibiting *S. mutans* growth.

CPNs-exposed *S. mutans* presented an elongated cell morphology when compared with bacteria incubated in water (Fig. 4). In addition to the elongated morphology, some constrictions along the bacteria were observed, and these constrictions may represent Z-

rings. The tubulin homolog filamenting temperature-sensitive mutant Z (FtsZ), which polymerizes at the midcell into a ring-like structure called the Z-ring[33], has a significant role in coordinating Z-ring formation because FtsZ recruits directly or indirectly various division proteins to the division site, including some of the penicillin-binding proteins and cell wall hydrolases[34-38]. The Z-ring is thought to function as a cytoskeletal element analogous to the contractile ring in many eukaryotic cells. Evidence suggests that all prokaryotic organisms use the Z-ring for division[39]. Thus, assembly and stability of the Z-ring are essential for proper division. The odd number of Z-rings would lead to abnormal bacterial division.

Additionally, remodeling of Z-rings in bacteria is associated with their cell cycle, and abnormal formation of Z-rings may lead to cell death[40, 41]. Therefore, in our study, the presence of Z-rings along *S. mutans* exposed to CPNs may be caused by abnormal division or cell death. The presence of Z-rings and the death of *S. mutans* were prominent when the bacteria were exposed to PAA-Pt nanoparticles. Further research should be conducted at a genetic level to address the structure of Z-rings.

A relevant to arrest existing carious lesions is biofilm control[3]. However, bacteria in biofilms display lower susceptibility to antibacterial agents when compared with that of planktonic bacteria[42]. In the present study, PAA-Pt disrupted the formation of biofilms with higher activity than the other two CPN formulations examined (Figs. 5–7). Similar results were observed for the live/dead cell staining experiments and SEM observations. Disruption of biofilm in the presence of 0.5 mM PAA-Pt was more prominent than that observed for the other CPNs at 0.5 mM. As mentioned earlier, CPNs enhanced the

bonding performance of 4-META/MMA-TBB-based resin cement[22-24]. Therefore, the PAA-Pt might also be a potential candidate for the adhesive dental materials. Recently, caries treatment with less surgical intervention has been described as essential for teeth preservation over time, as per the leading principle of minimal intervention dentistry[43]. Reducing cariogenic bacteria to eliminate the risk of further demineralization and cavitation is essential in minimal intervention dentistry. Thus, adhesive materials containing CPNs in their formulations with antibacterial properties can be promising for minimal intervention dentistry.

CONCLUSION

All three types of colloidal platinum nanoparticles prepared were found to inhibit *S. mutans* growth and biofilm formation. These results indicate that colloidal platinum nanoparticles represent a promising antibacterial agent to use in conjunction with adhesive materials for dental caries prevention around restorations.

ACKNOWLEDGMENTS

The authors acknowledge the support from Apt company for providing the colloidal platinum nanoparticles solutions. Technical support from the Department of Vascular Biology and Molecular Pathology is gratefully appreciated. The Japan Society funded this study for the Promotion of Science (20K09917 and 19K10123).

REFERENCES

1) Takahashi N, Nyvad B. Ecological hypothesis of dentin and root caries. Caries research. 2016;50(4):422-31.
2) Valdebenito B, Tullume-Vergara PO, Gonzalez W, Kreth J, Giacaman RA. In silico analysis of the competition between Streptococcus sanguinis and Streptococcus mutans in the dental biofilm. Molecular oral microbiology. 2018 Apr;33(2):168-80.
3) Schwendicke F, Splieth C, Breschi L, Banerjee A, Fontana M, Paris S, Burrow MF, Crombie F, Page LF, Gatón-Hernández P, Giacaman R. When to intervene in the caries process? An expert Delphi consensus statement. Clinical oral investigations. 2019 Oct;23(10):3691-703.
4) Schwendicke F, Splieth CH, Bottenberg P, Breschi L, Campus G, Doméjean S, Ekstrand K, Giacaman RA, Haak R, Hannig M, Hickel R. How to intervene in the caries process in adults: proximal and secondary caries? An EFCD-ORCA-DGZ expert Delphi consensus statement. Clinical oral investigations. 2020 Sep;24(9):3315-21.
5) Alves LV, Curylofo-Zotti FA, Borsatto MC, de Souza Salvador SL, Valério RA, Souza-Gabriel AE, Corona SA. Influence of antimicrobial photodynamic therapy in carious lesion. Randomized split-mouth clinical trial in primary molars. Photodiagnosis and photodynamic therapy. 2019 Jun 1;26:124-30.
6) Jiao Y, Tay FR, Niu LN, Chen JH. Advancing antimicrobial strategies for managing oral biofilm infections. International journal of oral science. 2019 Oct 1;11(3):1-1.
7) Zhou Y, Hiraishi N, Shimada Y, Wang G, Tagami J, Feng X. Evaluation of tooth demineralization and interfacial bacterial penetration around resin composites

containing surface pre-reacted glass-ionomer (S-PRG) filler. Dental Materials. 2021 May 1;37(5):849-62.

8) Elsaka SE, Hamouda IM, Swain MV. Titanium dioxide nanoparticles addition to a conventional glass-ionomer restorative: influence on physical and antibacterial properties. Journal of dentistry. 2011 Sep 1;39(9):589-98.

9) Cheng L, Weir MD, Xu HH, Antonucci JM, Kraigsley AM, Lin NJ, Lin-Gibson S, Zhou X. Antibacterial amorphous calcium phosphate nanocomposites with a quaternary ammonium dimethacrylate and silver nanoparticles. Dental Materials. 2012 May 1;28(5):561-72.

10) Argueta-Figueroa L, Scougall-Vilchis RJ, Morales-Luckie RA, Olea-Mejia OF. An evaluation of the antibacterial properties and shear bond strength of copper nanoparticles as a nanofiller in orthodontic adhesive. Australian orthodontic journal. 2015 May;31(1):42-8.

11) Hernández-Sierra JF, Ruiz F, Pena DC, Martínez-Gutiérrez F, Martínez AE, Guillén AD, Tapia-Pérez H, Castañón GM. The antimicrobial sensitivity of Streptococcus mutans to nanoparticles of silver, zinc oxide, and gold. Nanomedicine: Nanotechnology, Biology and Medicine. 2008 Sep 1;4(3):237-40.

12) Singh G, Joyce EM, Beddow J, Mason TJ. Evaluation of antibacterial activity of ZnO nanoparticles coated sonochemically onto textile fabrics. Journal of microbiology, biotechnology and food sciences. 2021 Jan 6;2021:106-20.

13) Holister P, Weener JW, Roman C, Harper T. Nanoparticles. Technology white papers. 2003 Oct;3:1-1.

14) Chwalibog A, Sawosz E, Hotowy A, Szeliga J, Mitura S, Mitura K, Grodzik M, Orlowski P, Sokolowska A. Visualization of interaction between inorganic nanoparticles and bacteria or fungi. International Journal of Nanomedicine. 2010;5:1085.

15) Tahir K, Nazir S, Ahmad A, Li B, Khan AU, Khan ZU, Khan FU, Khan QU, Khan A, Rahman AU. Facile and green synthesis of phytochemicals capped platinum nanoparticles and in vitro their superior antibacterial activity. Journal of Photochemistry and Photobiology B: Biology. 2017 Jan 1;166:246-51.

16) HASHIMOTO M, YANAGIUCHI H, KITAGAWA H, HONDA Y. Inhibitory effect of platinum nanoparticles on biofilm formation of oral bacteria. Nano Biomedicine. 2017;9(2):77-82.

17) Onizawa S, Aoshiba K, Kajita M, Miyamoto Y, Nagai A. Platinum nanoparticle antioxidants inhibit pulmonary inflammation in mice exposed to cigarette smoke. Pulmonary pharmacology & therapeutics. 2009 Aug 1;22(4):340-9.

18) Yoshihisa Y, Honda A, Zhao QL, Makino T, Abe R, Matsui K, Shimizu H, Miyamoto Y, Kondo T, Shimizu T. Protective effects of platinum nanoparticles against UV‐light‐induced epidermal inflammation. Experimental dermatology. 2010 Nov;19(11):1000-6.

19) Yoshihisa Y, Zhao QL, Hassan MA, Wei ZL, Furuichi M, Miyamoto Y, Kondo T, Shimizu T. SOD/catalase mimetic platinum nanoparticles inhibit heat-induced apoptosis in human lymphoma U937 and HH cells. Free radical research. 2011 Mar 1;45(3):326-35.

20) Watanabe A, Kajita M, Kim J, Kanayama A, Takahashi K, Mashino T, Miyamoto Y. In vitro free radical scavenging activity of platinum nanoparticles. Nanotechnology. 2009 Oct 16;20(45):455105.

21) Elkassas D, Arafa A. The innovative applications of therapeutic nanostructures in dentistry. Nanomedicine: Nanotechnology, Biology and Medicine. 2017 May 1;13(4):1543-62.

22) Nagano F, Selimovic D, Noda M, Ikeda T, Tanaka T, Miyamoto Y, Koshiro KI, Sano H. Improved bond performance of a dental adhesive system using nano-technology. Bio-medical materials and engineering. 2009 Jan 1;19(2-3):249-57.

23) Hoshika S, Nagano F, Tanaka T, Ikeda T, Wada T, Asakura K, Koshiro K, Selimovic D, Miyamoto Y, Sidhu SK, Sano H. Effect of application time of colloidal platinum nanoparticles on the microtensile bond strength to dentin. Dental materials journal. 2010;29(6):682-9.

24) Hoshika S, Nagano F, Tanaka T, Wada T, Asakura K, Koshiro K, Selimovic D, Miyamoto Y, Sidhu SK, Sano H. Expansion of nanotechnology for dentistry: effect of colloidal platinum nanoparticles on dentin adhesion mediated by 4-META/MMA-TBB. The journal of adhesive dentistry. 2011 Oct;13(5):411-6.

25) Joves GJ, Inoue G, Sadr A, Nikaido T, Tagami J. Nanoindentation hardness of intertubular dentin in sound, demineralized and natural caries-affected dentin. journal of the mechanical behavior of biomedical materials. 2014 Apr 1;32:39-45.

26) Sato Y, Yamamoto Y, Kizaki H. Cloning and sequence analysis of the gbpC gene encoding a novel glucan-binding protein of Streptococcus mutans. Infection and immunity. 1997 Feb;65(2):668-75.

27) Liu R, Tang Y, Zeng L, Zhao Y, Ma Z, Sun Z, Xiang L, Ren L, Yang K. In vitro and in vivo studies of antibacterial copper-bearing titanium alloy for dental application. Dental Materials. 2018 Aug 1;34(8):1112-26.

28) Chen M, Zhang E, Zhang L. Microstructure, mechanical properties, bio-corrosion properties and antibacterial properties of Ti–Ag sintered alloys. Materials Science and Engineering: C. 2016 May 1;62:350-60.

29) Christensen GD, Simpson WA, Younger JJ, Baddour LM, Barrett FF, Melton DM, Beachey EH. Adherence of coagulase-negative staphylococci to plastic tissue culture plates: a quantitative model for the adherence of staphylococci to medical devices. Journal of clinical microbiology. 1985 Dec;22(6):996-1006.

30) Holečková N, Doubravová L, Massidda O, Molle V, Buriánková K, Benada O, Kofroňová O, Ulrych A, Branny P. LocZ is a new cell division protein involved in proper septum placement in Streptococcus pneumoniae. MBio. 2014 Dec 30;6(1):e01700-14.

31) Smith JJ, Wayman BE. An evaluation of the antimicrobial effectiveness of citric acid as a root canal irrigant. Journal of endodontics. 1986 Jan 1;12(2):54-8.

32) Yamaguchi M, Yoshida K, Suzuki R, Nakamura H. Root canal irrigation with citric acid solution. Journal of endodontics. 1996 Jan 1;22(1):27-9.

33) Haeusser DP, Margolin W. Splitsville: structural and functional insights into the dynamic bacterial Z ring. Nature Reviews Microbiology. 2016 May;14(5):305-19.

34) Sham LT, Tsui HC, Land AD, Barendt SM, Winkler ME. Recent advances in pneumococcal peptidoglycan biosynthesis suggest new vaccine and antimicrobial targets. Current opinion in microbiology. 2012 Apr 1;15(2):194-203.

35) Egan AJ, Vollmer W. The physiology of bacterial cell division. Annals of the New York Academy of Sciences. 2013 Jan;1277(1):8-28.

36) Massidda O, Nováková L, Vollmer W. From models to pathogens: how much have we learned about Streptococcus pneumoniae cell division?. Environmental microbiology. 2013 Dec;15(12):3133-57.

37) Fleurie A, Manuse S, Zhao C, Campo N, Cluzel C, Lavergne JP, Freton C, Combet C, Guiral S, Soufi B, Macek B. Interplay of the serine/threonine-kinase StkP and the paralogs DivIVA and GpsB in pneumococcal cell elongation and division. PLoS genetics. 2014 Apr 10;10(4):e1004275.

38) Jacq M, Arthaud C, Manuse S, Mercy C, Bellard L, Peters K, Gallet B, Galindo J, Doan T, Vollmer W, Brun YV. The cell wall hydrolase Pmp23 is important for assembly and stability of the division ring in Streptococcus pneumoniae. Scientific reports. 2018 May 15;8(1):1-4.

39) Lutkenhaus J, Addinall SG. Bacterial cell division and the Z ring. Annual review of biochemistry. 1997 Jul;66(1):93-116.

40) Palmer SR, Ren Z, Hwang G, Liu Y, Combs A, Söderström B, Lara Vasquez P, Khosravi Y, Brady LJ, Koo H, Stoodley P. Streptococcus mutans yidC1 and yidC2

impact cell envelope biogenesis, the biofilm matrix, and biofilm biophysical properties. Journal of bacteriology. 2019 Jan 1;201(1):e00396-18.

41) Jacq M, Adam V, Bourgeois D, Moriscot C, Di Guilmi AM, Vernet T, Morlot C. Remodeling of the Z-ring nanostructure during the Streptococcus pneumoniae cell cycle revealed by photoactivated localization microscopy. MBio. 2015 Aug 18;6(4):e01108-15.

42) Drenkard E. Antimicrobial resistance of Pseudomonas aeruginosa biofilms. Microbes and infection. 2003 Nov 1;5(13):1213-9.

43) Tyas MJ, Anusavice KJ, Frencken JE, Mount GJ. Minimal intervention dentistry—a review* FDI Commission Project 1–97. International dental journal. 2000 Feb;50(1):1-2.

Figure legends

Table 1 The composition of the three types of CPNs

Product	Lot No.	Composition	pH value
PAA-Pt	111170908	Pt (platinum): 0.02%, 1 mM PAA (polyacrylic acid): 1.16% Water: 98.82%	6.40
C-Pt	331180316	Pt (platinum): 0.02%, 1mM Sodium citric acid: 0.29% Water: 99.69%	6.12
C-CyD-Pt	251180316	Pt (platinum): 0.02%, 1mM Sodium citric acid: 0.29%, Cyclodextrin: 0.3% Water: 99.39%	6.10
Three types of CPNs are provided by Apt company (Tokyo, Japan).			

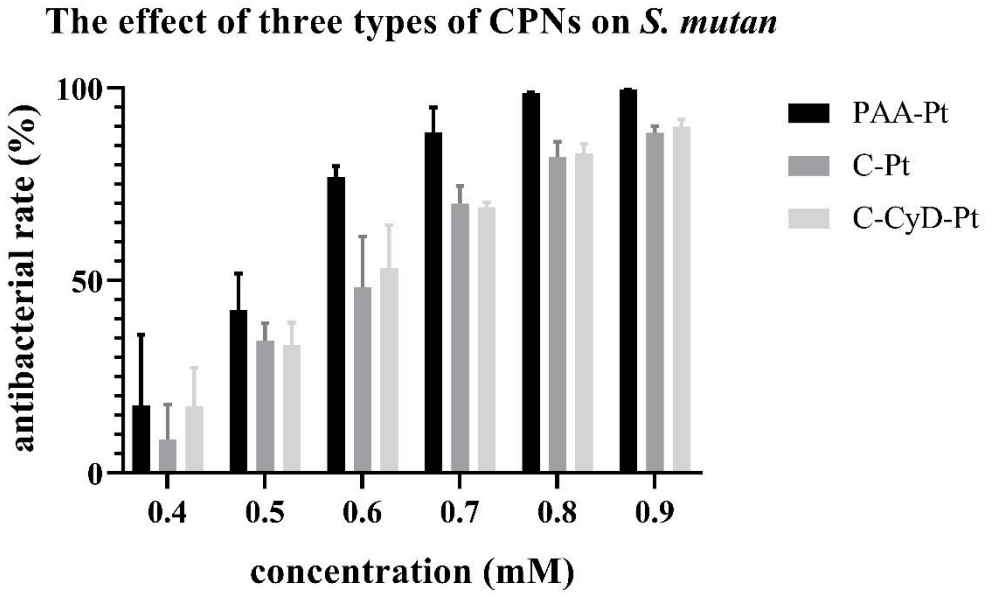

Fig. 1 Antibacterial rate assay for the three CPNs groups.

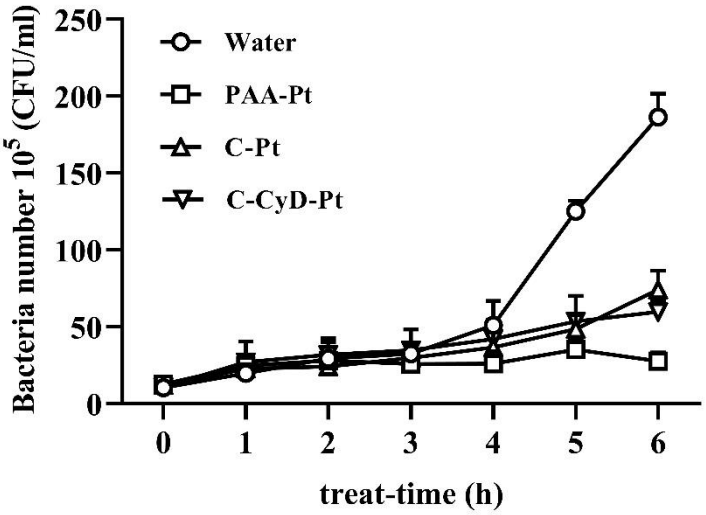

Fig. 2 Growth inhibition assay of bacteria. The number of bacteria at different treatment times (0–6 h) for the four groups were examined. The concentration of each CPNs group was 0.7 mM.

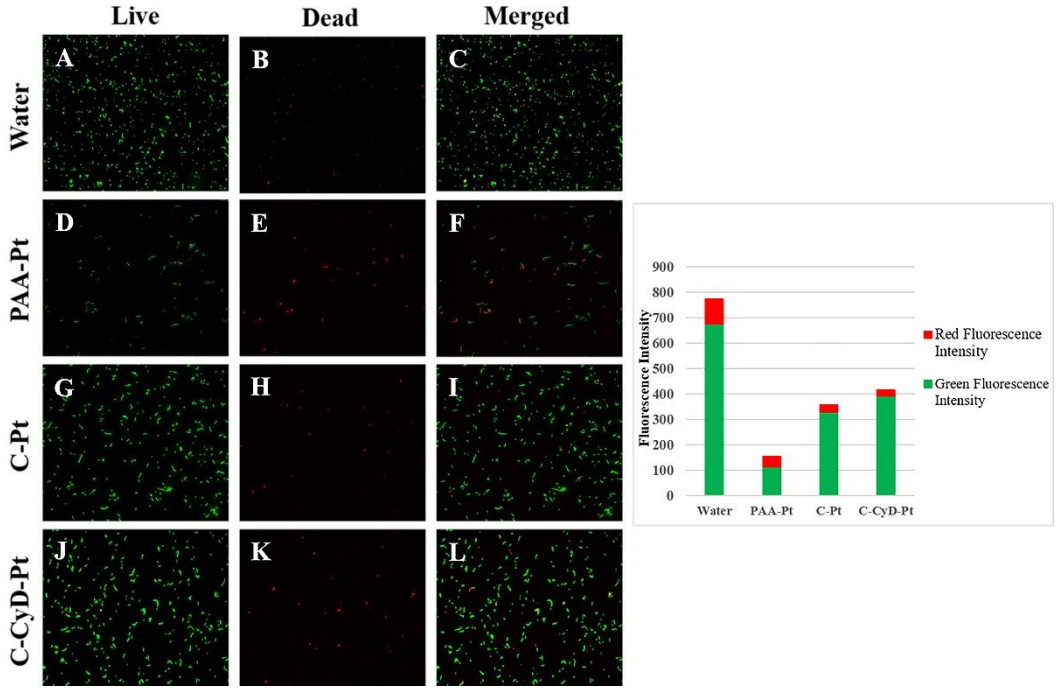

Fig. 3 Representative live/dead staining images of *S. mutans* treated with CPNs (concentration of CPNs: 0.7 mM; treatment period: 24 h). Live bacteria are stained green, whereas dead bacteria are stained red. Magnification: ×200.

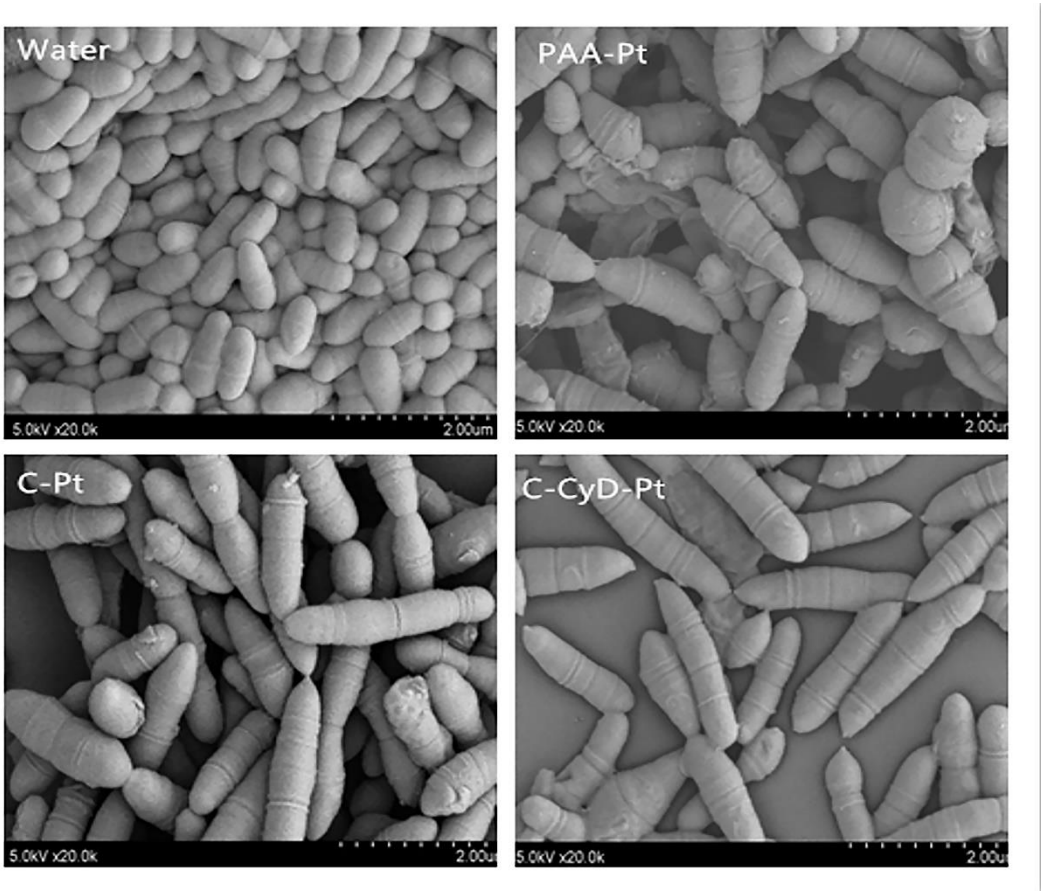

Fig. 4 Representative SEM images of *S. mutans* treated with CPNs (concentration: 0.7 mM; treatment period: 24 h).

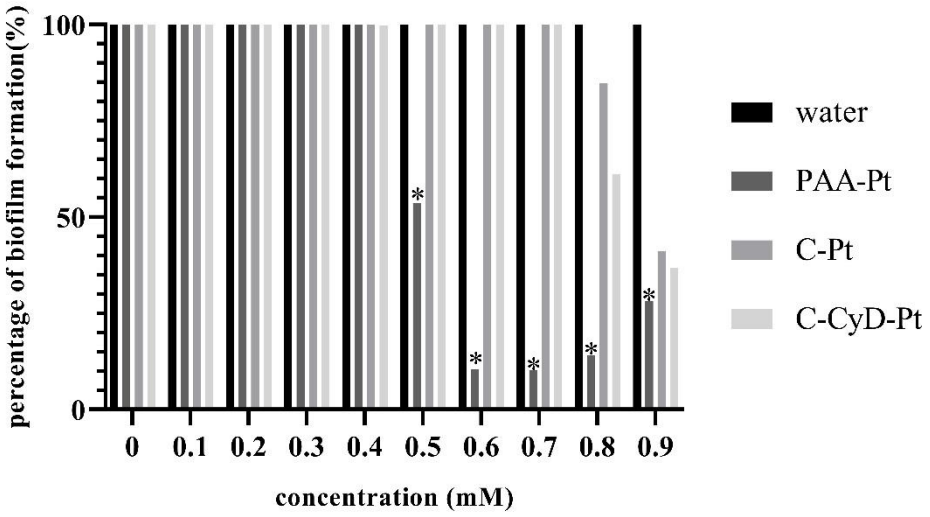

Fig. 5 Inhibition of bacterial biofilm formation by CPNs. * indicates statistically significant difference.

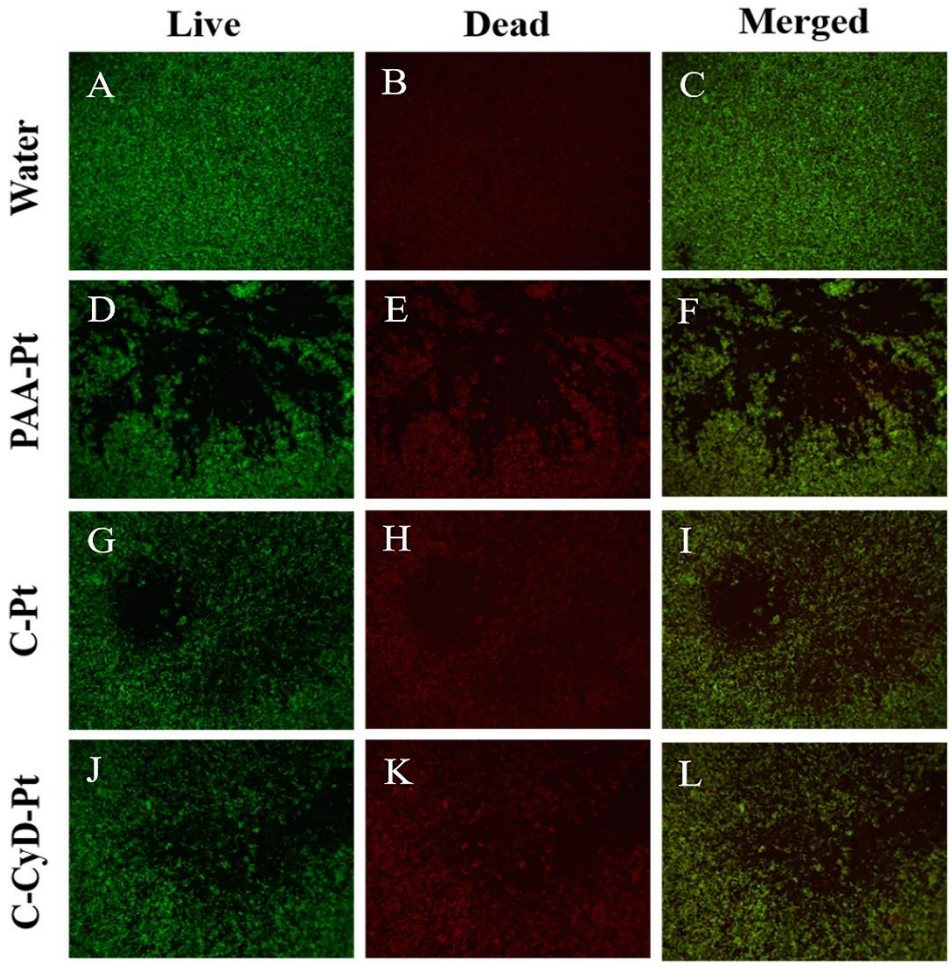

Fig. 6 Representative live/dead staining images of *S. mutans* biofilm formation treated with CPNs (concentration: 0.5 mM, treatment period: 24 h). Live bacteria are stained green and dead bacteria are stained red. Magnification: ×200.

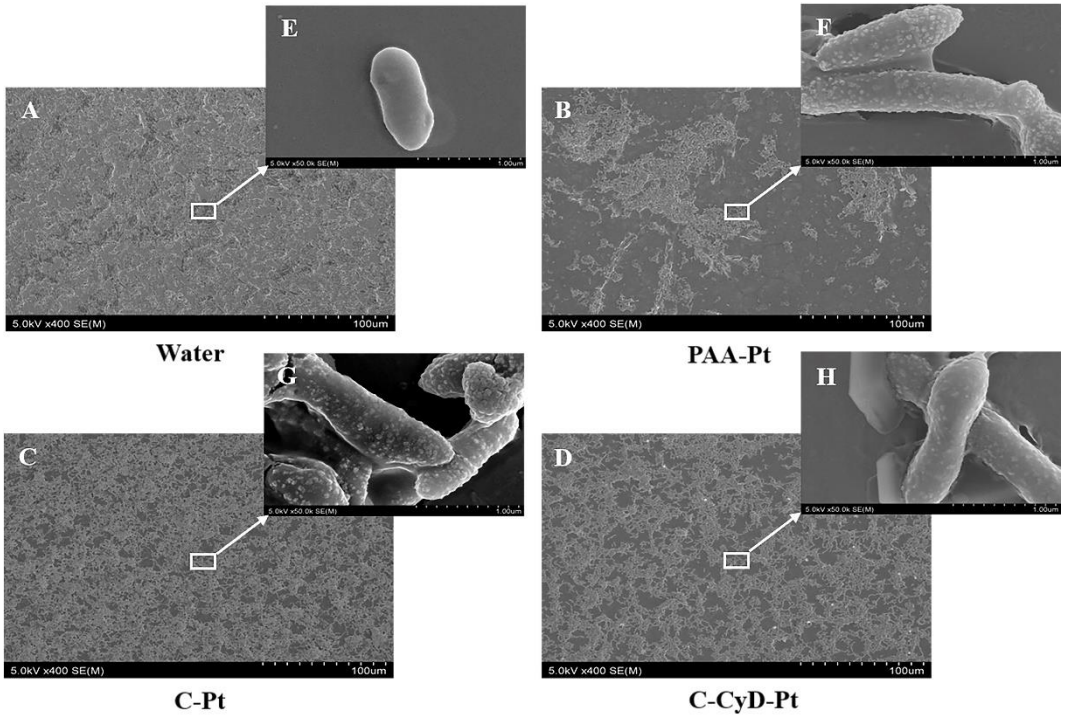

Fig. 7 Representative SEM images of *S. mutans* biofilm formation treated with CPNs (concentration: 0.5 mM; treatment period: 24 h).